Neuro-Oncology
19(2), 175–185, 2017 | doi:10.1093/neuonc/now147 | Advance Access date 14 July 2016

ELTD1, an effective anti-angiogenic target for gliomas: preclinical assessment in mouse GL261 and human G55 xenograft glioma models

Jadith Ziegler, Richard Pody, Patricia Coutinho de Souza, Blake Evans, Debra Saunders, Nataliya Smith, Samantha Mallory, Charity Njoku, Yunzhou Dong, Hong Chen, Jiali Dong, Megan Lerner, Osamah Mian, Sai Tummala, James Battiste, Kar-Ming Fung, Jonathan D. Wren, and Rheal A. Towner

Advanced Magnetic Resonance Center, Oklahoma Medical Research Foundation, Oklahoma City, Oklahoma (J.Z., R.P., P.C.d.S., B.E., D.S., N.S., S.M., C.N., J.D., O.M., R.A.T.); Comparative Medicine, Oklahoma Medical Research Foundation, Oklahoma City, Oklahoma (S.T.); Arthritis and Clinical Immunology, Oklahoma Medical Research Foundation, Oklahoma City, Oklahoma (J.D.W.); Vascular Biology Program, Boston Children's Hospital and Harvard Medical School, Karp Family Research Laboratories, Boston, Massachusetts (Y.D., H.C.); Department of Pathology, Oklahoma City, Oklahoma (J.Z., K.-M.F., R.A.T.); Department of Biochemistry and Molecular Biology, Oklahoma City, Oklahoma (J.D.W.); Department of Surgery Research Laboratory, Oklahoma City, Oklahoma (M.L.); The Stephenson Cancer Center, Oklahoma City, Oklahoma (J.B., K.-M.F., R.A.T.); The University of Oklahoma Children's Hospital, University of Oklahoma Health Sciences Center, Oklahoma City, Oklahoma (S.M.)

Corresponding Author: Rheal A. Towner, PhD, Advanced Magnetic Resonance Center, Oklahoma Medical Research Foundation, 825 NE 13th Street, Oklahoma City, OK 73104 (rheal-towner@omrf.org).

Abstract

Background. Despite current therapies, glioblastoma is a devastating cancer, and validation of effective biomarkers for it will enable better diagnosis and therapeutic intervention for this disease. We recently discovered a new biomarker for high-grade gliomas, ELTD1 (epidermal growth factor, latrophilin, and 7 transmembrane domain-containing protein 1 on chromosome 1) via bioinformatics, and validated that ELTD1 protein levels are significantly higher in human and rodent gliomas. The focus of this study was to assess the effect on tumor growth of an antibody against ELTD1 in orthotopic, GL261, and G55 xenograft glioma models.

Methods. The effect of anti-ELTD1 antibody therapy was assessed by animal survival, MRI measured tumor volumes, MR angiography, MR perfusion imaging, and immunohistochemistry (IHC) characterization of microvessel density in mouse glioma models. Comparative treatments included anti–vascular endothelial growth factor (VEGF) and anti–c-Met antibody therapies, compared with untreated controls.

Results. Tumor volume and survival data in this study show that antibodies against ELTD1 inhibit glioma growth just as effectively or even more so compared with other therapeutic targets studied, including anti-VEGF antibody therapy. Untreated GL261 or G55 tumors were found to have significantly higher ELTD1 levels (IHC) compared with contralateral normal brain. The anti-angiogenic effect of ELTD1 antibody therapy was observed in assessment of microvessel density, as well as from MR angiography and perfusion measurements, which indicated that anti-ELTD1 antibody therapy significantly decreased vascularization compared with untreated controls.

Conclusions. Either as a single therapy or in conjunction with other therapeutic approaches, anti-ELTD1 antibodies could be a valuable new clinical anti-angiogenic therapeutic for high-grade gliomas.

Key words

anti-ELTD1 antibody | ELTD1 ([epidermal growth factor (EGF), GL261 and G55 gliomas, latrophilin and seven transmembrane domain-containing 1] on chromosome 1) | MRI

High-grade gliomas (World Health Organization grades III/IV) are the most common primary brain tumors in adults, and their malignant nature ranks them fourth in incidence of cancer death.[1–5] Approximately 15 000 patients die of glioblastomas in the US annually.[1–4] Malignant brain tumors kill ~140 000 people worldwide per year.[6] Standard treatment for glioblastoma, which typically involves surgical resection followed by a combination of radiation and chemotherapy with temozolomide, has not improved overall survival (median survival remains 15–18 mo; 5-y survival rates are <10%).[7,8] Prognosis is even poorer for recurrent disease, with response rates for cytotoxic chemotherapy typically in the range of 5%–10%, and a 6-month progression-free survival rate of <15%.[8,9] One therapeutic strategy being actively pursued for multiple cancers is targeting angiogenesis, because without the ability to vascularize, a tumor cannot grow in size.

Angiogenesis is greatly upregulated in high-grade gliomas compared with low-grade gliomas[10] and is an essential process that provides excess nutrients to developing tumors even at very early stages.[11] Assessing angiogenesis is one of the most important criteria for grading tumors in patients.[12] In addition to cytotoxic chemotherapy, bevacizumab (Avastin), an anti–vascular endothelial growth factor (VEGF) antibody therapeutic, is used to inhibit angiogenesis as a treatment for recurrent glioblastoma but has not significantly improved clinical outcome.[7,10]

Antibody development is a well-established technology, with the rate-limiting step in developing antibody-based or biological therapeutics being identification of target proteins to be inhibited. Molecular markers have increasingly been used to assess and manage adult malignant gliomas.[5,13–17] Dozens of proteomics-based approaches have sought to find proteins that are unique to gliomas[11] but have been severely limited by issues of sample size, ability to detect low abundance proteins, and reproducibility. Many of these studies have generated hundreds and even thousands of putative candidates, yet have not been able to follow them up with subsequent validation and characterization. Alternatively, a bioinformatics approach called global microarray meta-analysis (GAMMA) can be used to interpret empirical patterns from high-throughput data mining of transcriptional expression databases (>75 000 human microarray experiments) by using reported associations within the peer-reviewed literature (>24 million papers) to identify and prioritize uncharacterized proteins for their putative involvement in diseases.[18] Whether phenotype or disease relevance for a gene is known or not, a gene can be analyzed indirectly via its highly correlated transcriptional partners.[19,20] To identify novel genes associated with gliomas, we can search for all genes that are highly correlated with genes that are already known to be associated with gliomas in the peer-reviewed literature. Using the Human Proteome Reference Database[21] and other experimental sources on protein subcellular localizations, a list of predicted glioma-associated proteins can be screened for those that are likely to be expressed on the plasma membrane. Our initial motivation was to identify novel glioma biomarkers, in the hopes that they would be of value for clinical diagnostics, prognostics, or therapeutics. We have validated 6 novel biomarkers specific to gliomas that were identified via the GAMMA bioinformatics approach.[22,23] The first of these validated biomarkers was *epidermal growth factor, latrophilin, and 7 transmembrane domain-containing protein 1 on chromosome 1* (ELTD1), which we found to be highly enriched in the angiogenic regions of gliomas.[22]

To our knowledge, this was the first time that surface biomarkers of gliomas were identified by purely computational means.[22] ELTD1 has been reported as an endothelial marker in microvasculature.[24] In our previous study, ELTD1 was significantly higher ($P = .03$) in high-grade gliomas (50 patients) compared with low-grade gliomas (21 patients), and this marker compared well with traditional immunohistochemical (IHC) markers used to identify high-grade glioma tissue including VEGF, glucose transporter 1, carbonic anhydrase 9, and hypoxia-inducible factor–1α.[22] ELTD1 gene expression was correlated with tumor grade, survival across grades, and an increase in the mesenchymal subtype.[22] In a rat F98 glioma model, co-localization images stained for ELTD1 and cluster of differentiation (CD)31 indicated that most of the ELTD1 detected by fluorescence confocal imaging was associated with endothelial cells. Specificity of the ELTD1 probe seems to be in areas associated with neovascularization.[22]

In this study, we investigated the potential of ELTD1 as an anticancer target via the use of an anti-ELTD1 antibody as a potential therapy in orthotopic mouse GL261 and human G55 xenograft glioma preclinical models. Morphological MRI was used to calculate tumor volumes. Other comparative anticancer therapies included anti-VEGF and/or anti–c-Met antibodies. In addition to tumor volumes, percent animal survival was assessed, as well as IHC evaluation of ELTD1 and CD34 levels. CD34 IHC was used to calculate microvessel densities (MVDs) as a measure of angiogenesis.

Methods

Glioma Models

Two-month-old male C57BL6/J mice or Hsd:Athymic Nude-Foxn1nu mice (Harlan) were intracerebrally implanted with either mouse GL261 (10^4) or human G55 (10^5) glioma cells, respectively, as previously done.[24–26]

Treatments

GL261 tumor-bearing mice (n = 4–7 per group) were treated with either anti-ELTD1 (ELT, N-20, goat polyclonal [#sc-46951, Santa Cruz Tech]; 2 mg/kg in 100 μL saline every 3 days for up to tumor maximum), anti-VEGF (mouse monoclonal antibody; 1.5–2.0 mg/kg in 100 μL saline every 3 days for up to tumor maximum [Genentech]), or anti–c-Met antibodies (c-Met, B-2, mouse monoclonal [#sc-8057, Santa Cruz Tech]; 1 mg/kg in 100 μL saline every 3 days for up to tumor maximum). Untreated mice served as controls for statistical comparison. G55 tumor-bearing mice (n = 5–7/group) were treated with either anti-ELTD1 (same as GL261 model) or anti-VEGF (bevacizumab; Avastin, Genentech), or nonspecific mouse immunoglobulin (Ig)G as antibody control (Alpha Diagnostics), or were untreated controls.

Treatments were started when tumors reached 10–20 mm^3 in volume. All antibody treatments were administered via a tail vein catheter. All animal studies were approved by the Oklahoma Medical Research Foundation Institutional Animal Care and Use Committee. Animal percent survivals were obtained, with the proviso that all mice were euthanized when tumor volumes reached ≥150 mm^3.

MRI

MRI experiments were performed on a Bruker BioSpec 7.0 Tesla/30-cm horizontal-bore magnet imaging system. Animals were immobilized by using 1.5%–2.5% isoflurane and 0.8 L/min O_2 and placed in a 72-mm quadrature volume coil for signal transmission, and a surface mouse-head coil was used for signal reception. T2-weighted imaging was acquired as previously done by our group.[22,24–26] Tumor volumes were calculated from 3D MRI slices rendered MRI datasets, using Amira v5.6.0 (FEI).

MR Angiography

MR angiography (MRA) was used to obtain macrovascular images (tumor blood vessels >50 μm in diameter) in the GL261 model as previously described.[24] Briefly, MRA data were acquired within a volume-of-interest of 1.28 × 1 × 0.64 cm^3, at an angle of 16 degrees relative to the horizontal plane, and a flip angle of 90 degrees, for a total acquisition time of 25 min.[24] Tumor blood volumes were segmented from 3D MR angiograms and quantified using Mathematica.[23] Datasets were reconstructed to provide a pixel resolution of 50 × 78 × 100 μm^3.[24] For analysis, a region of interest (ROI) encompassing blood vessels in the tumor area was selected and used to provide absolute tumor blood volumes.[24]

Perfusion Imaging

In order to assess microvascular alterations associated with tumor capillaries, the perfusion imaging method, arterial spin labeling, was used as previously described.[25,26] Perfusion maps were obtained on a single axial slice of the brain located on the point of the rostro-caudal axis where the tumor had the largest cross section.[25,26] The imaging geometry was a 3.5 × 3.5 mm^2 slice, of 1.5 mm in thickness, with a single shot echo-planar encoding over a 64 × 64 matrix. An echo time of 20 ms and a repetition time of 18 s were used. To obtain perfusion contrast, the flow alternating inversion recovery scheme was used, where inversion recovery images were acquired using selective and nonselective slices. For each type of inversion, 8 images were acquired with inversion times evenly spaced at 20–2820 ms. For perfusion data, the recovery curves obtained from each pixel for nonselective or selective inversion images were numerically fitted to derive pixelwise T_1 and T_1* values, respectively, and longitudinal recovery rates were then used to calculate the cerebral blood flow, *CBF* (mL/(100 g·min)), from: CBF=λ[(1/T1*)–(1/T1)].[27] The partition coefficient, λ, was scaled by the value of 0.9 mL/g.[28] To calculate differences in relative (r)CBF values, tumor rCBF values were obtained at late tumor stages (days 18–26 following i.c. implantation of GL261 cells, or after tumor detection for G55 cells, for untreated mice, and days 20–31 [after GL261 implantation or G55 tumor detection] for treated mice) and early tumor stages (days 10–13 following GL261 cell implantation or G55 tumor detection) and were normalized to rCBF values in the contralateral brain region of corresponding animals.

Histology and Immunohistochemistry

All mice were euthanized after the last MRI examination. Perfusion fixation (10% neutral buffered formalin administered via a tail vein injection) was used on anesthetized (isoflurane) mice, and whole brain of each animal was removed, further preserved in 10% neutral buffered formalin, and processed routinely. Paraffin-embedded tissues were sectioned at 5 μm, mounted on SuperFrost Plus glass slides (Fisher Scientific), stained with hematoxylin and eosin, and examined by light microscopy. Iron Staining Kit (Ventana Medical Systems) was used to stain for hemorrhaging. IHC was done to establish ELTD1 levels by staining tissue samples with anti-ELTD1 antibody (rabbit anti-ELT, 10 μg/mL; #ab150489, Abcam). For ELTD1 IHC, sections were incubated in an antigen retrieval solution (citrate buffer, pH 6; Vector Laboratories) for 20 min in a rice steamer, followed by a 20-min cooldown in deionized water. ELTD1 IHCs were analyzed using a Positive Pixel Count algorithm with the Aperio ImageScope viewer. Only areas containing tumor tissue were analyzed for IHC expression. Areas without tumor tissue and areas with necrosis or significant artifacts (eg, tissue folding) were deselected and excluded from analysis. The number of positive pixels was divided by the total number of pixels (negative and positive) in the analyzed area. To characterize MVD and tumor cell invasion, respectively, in both untreated and treated groups, IHC for anti-CD34 antibody (rabbit anti-CD34, 10 μg/mL; #ab81289, Abcam) was performed using an automated immunostainer (Bond-III, Leica). Sections were incubated in an antigen retrieval solution, as described above for ELTD1 IHC. Three ROIs with the highest number of blood vessels (200× magnification) were identified in each case. The MVD measurements were captured digitally for each selected ROI and calculated using the Aperio ScanScope Image Analysis System.[29]

Western Blot

Tissue and cell lysates were prepared in radioimmunoprecipitation assay buffer, mixed with loading buffer, heated, and loaded (12.5 μg/well) within a Mini-PROTEAN TGX Precast gradient gel 4%–15% (Bio-Rad Laboratories). The ELTD band was visualized using ELT (N-20; #sc-46951) antibody as a primary, and a secondary donkey anti-goat (#sc-2020) IgG–horseradish peroxidase.

Statistical Analysis

Statistical analyses were performed using ANOVA with a post Tukey's multiple comparison test for evaluating differences in tumor volumes between untreated and treated

groups. Data were represented as mean ± SD, and *P*-values <.05, <.01, and <.001 were considered statistically significant.

Results

We established initially whether GL261 or G55 tumors expressed high levels of ELTD1. ELTD1 IHC levels in untreated GL261 or G55 gliomas, compared with contralateral normal brain tissue, are depicted in Fig. 1. The levels of ELTD1 were significantly higher in tumor regions ($P < .0001$, GL261; $P < .01$, G55) compared with contralateral brain tissue (Fig. 1E and F, respectively). ELTD1 was found in high levels also in tumor and human vascular endothelial cells, as well as GL261 and G55 glioma cells (Fig. 1G). Due to the high levels of ELTD1 expression and its known role in angiogenesis, we then set out to

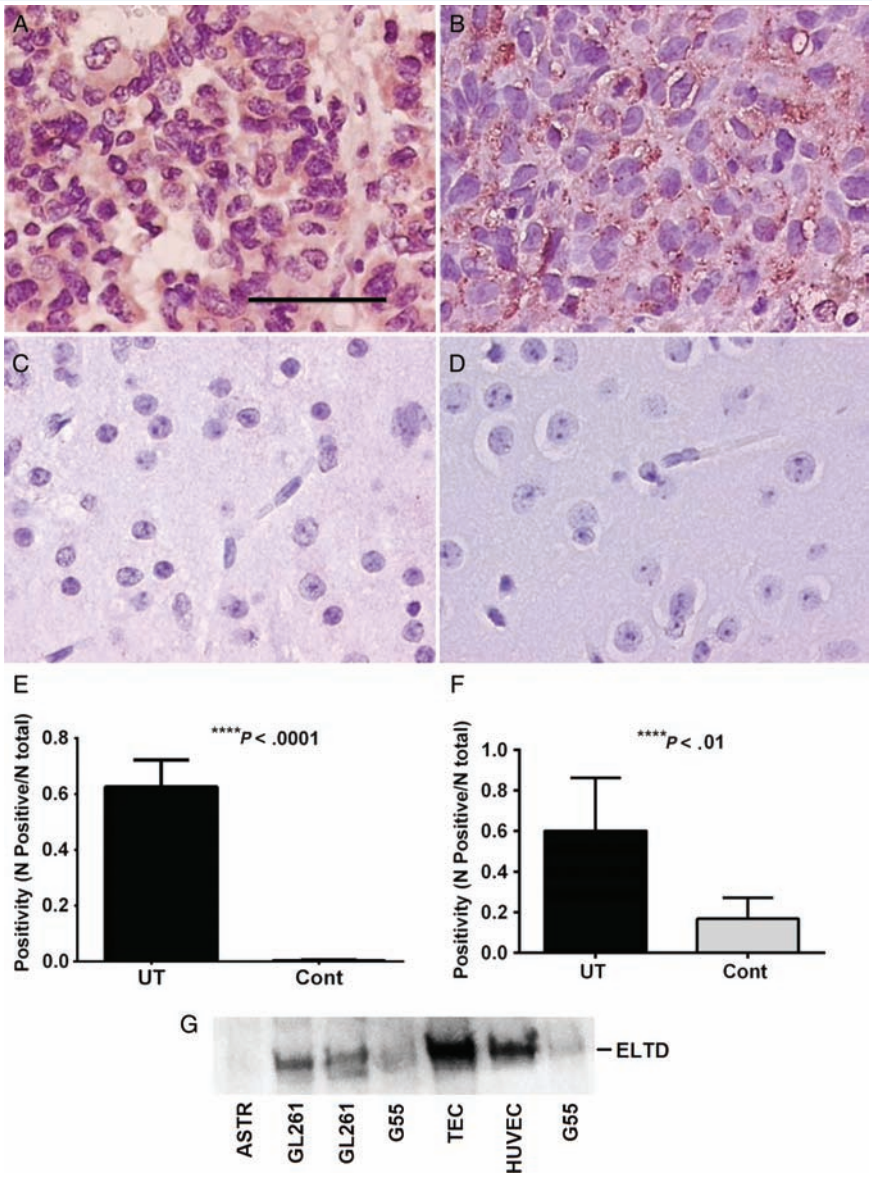

Fig. 1 ELTD1 is highly expressed in GL261 and G55 gliomas. Representative IHC for ELTD1 in untreated GL261 (A) and G55 (B) tumors; 20 × magnification. Representative IHC for ELTD1 in the contralateral normal brain region of GL261 (C) and G55 (D) tumor-bearing mice; 20 × magnification. ELTD1 staining (horseradish peroxidase) positivity (N positive/N total) in untreated (UT) GL261 (E) or G55 (F) tumors ($n = 5$ for each) compared with contralateral normal brain regions ($n = 7$ for each) (G) Western blot showing ELTD1 levels in primary astrocytes (ASTR), GL261 and G55 glioma cells, and tumor endothelial cells (TEC) or human umbilical vein endothelial cells (HUVEC). There was a significant increase in ELTD1 levels in GL261 ($P < .0001$) or G55 ($P < .01$) gliomas compared with normal contralateral brain tissue in each model. Magnification bar = 100 μm.

determine whether interfering with ELTD1 function via anti-ELTD1 antibody therapy would increase overall survival and decrease tumor volumes compared with untreated tumors.

We found that percent survival of GL261 and G55 glioma-bearing mice treated with anti-ELTD1 antibodies was significantly higher ($P < .01$ for both) compared with untreated and/or IgG-treated tumors, as depicted in Fig. 2A and G,

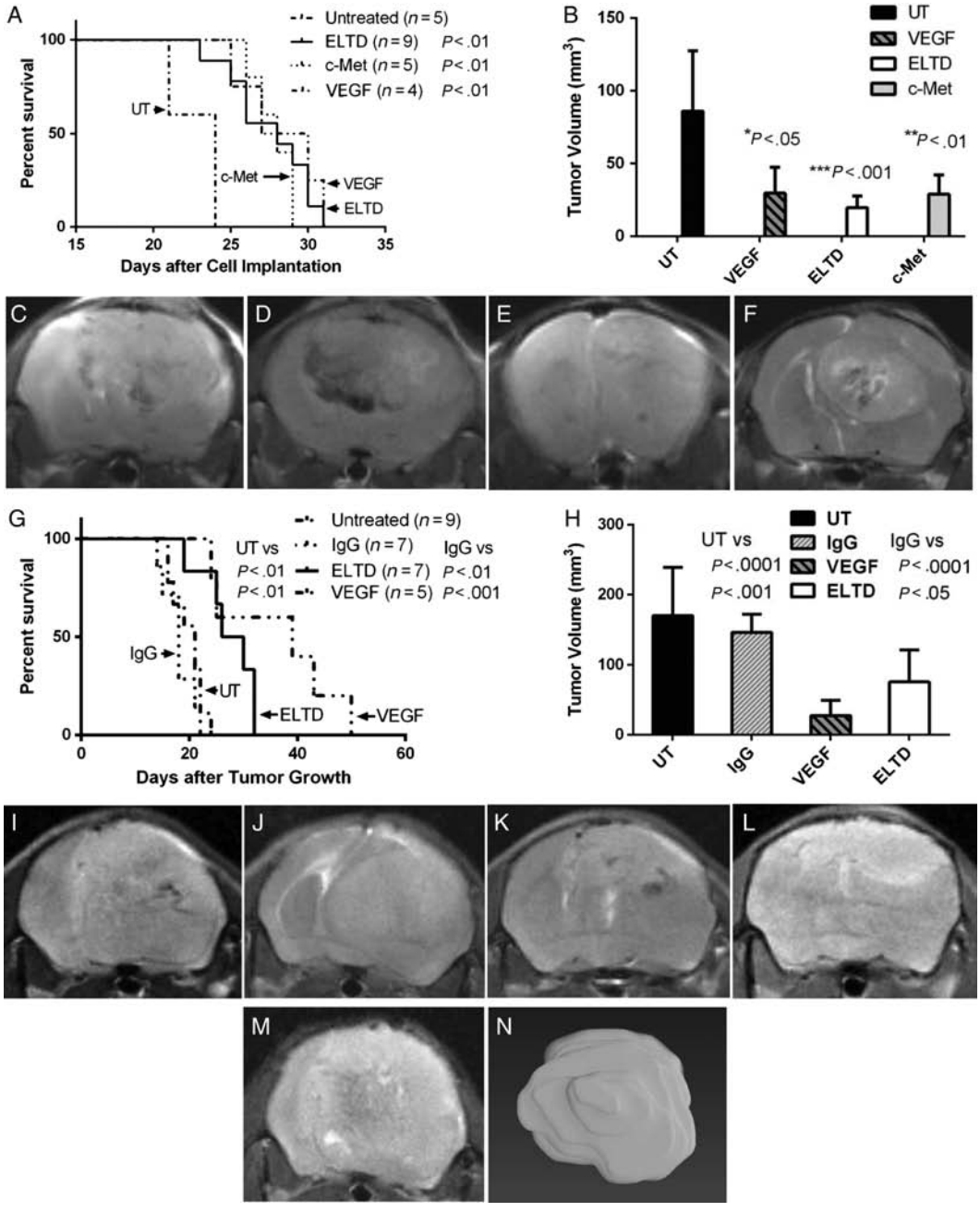

Fig. 2 Anti-ELTD1 antibody therapy increases animal survival and decreases tumor volumes in GL261 and G55 gliomas. Animal survival curves for GL261 (A) and G55 (G) glioma-bearing mice either untreated (UT) ($n = 5–9$) or treated with IgG ($n = 7$) or antibodies against either ELTD1 (ELTD) ($n = 7–9$), c-Met ($n = 5$), or VEGF ($n = 4–5$). There was a significant increase in survival for all treated groups ($P < .01$ for all treatment groups), compared with untreated mice. Tumor volumes (mm^3), measured from multiple MR image slices for either GL261 (B) or G55 (H) glioma mice, UT mice, or mice treated with IgG or antibodies against VEGF, ELTD1 (ELTD), or c-Met. There was a significant decrease in tumor volumes for all treated groups ($P < .05$ [GL261] or $P < .0001$ [G55] for VEGF, $P < .001$ [GL261] or $P < .001$ [G55] for ELTD, and $P < .01$ [GL261] for c-Met) compared with UT animals. Representative T2-weighted MRIs from GL261 (C–F) (21 days following GL261 cell implantation) or G55 (I–L) glioma-bearing mice either untreated (C or I), or treated with IgG (J) or antibodies against VEGF (D or K), ELTD1 (E or L), or c-Met (F). Tumor volumes obtained from T2-weighted image slices (M) that were 3D rendered (N).

respectively. Other antibody therapies, including anti-mouse anti-VEGF ($P < .01$, GL261; $P < .001$, G55) or anti–c-Met ($P < .01$ for GL261) antibodies also significantly increased animal survival compared with untreated GL261 (Fig. 2A) or IgG-treated or untreated G55 (Fig. 2G) gliomas. Tumor volumes at 21 days following intracerebral implantation of GL261 or 21 days after tumor detection for G55 cells were found to be significantly lower in anti-ELTD1 antibody-treated mice ($P < .001$ for both) compared with untreated controls or IgG-treated mice ($P < .05$, G55) (Fig. 2B and H, respectively). Likewise, anti-VEGF and anti–c-Met antibody treatments also had significantly decreased tumor volumes ($P < .05$ for anti-VEGF in GL261, $P < .0001$ for anti-VEGF in G55, and $P < .01$ for anti–c-Met in GL261) compared with untreated animals (Fig. 2B and H, respectively). Many of the untreated GL261 or untreated and IgG-treated G55 glioma-bearing mice were required to be euthanized, as tumor volumes reached ~150 mm^3 at the 21-day timepoint (following cell implantation for GL261 or after tumor detection for G55). Representative MRIs of GL261 tumor-bearing mice from all treatment groups are shown in Fig. 2C–F, whereas those from G55 tumor-bearing mice are shown in Fig. 2I–L. A representative 3D rendered tumor volume of the tumor from Fig. 2M is shown in Fig. 2N. We also noticed in the anti-VEGF–treated animals that several of the MRIs indicated hemorrhaging in the tumors (eg, Fig. 2D and K) compared with anti-ELTD1–treated (Fig. 2E and L) tumors. Histology (iron stain) was obtained to verify the hemorrhaging observed in the MRIs, particularly for the anti-VEGF–treated GL261 or G55 tumors. Figure 3 shows representative iron stained tumor tissues from each treatment group. Very little to no hemorrhaging is seen for the IgG-treated (Fig. 3A and D) or anti-ELTD1–treated (Fig. 3B and E) tumors compared with high areas of hemorrhaging seen for the anti-VEGF–treated tumors (Fig. 3C and Fi and Fii).

MVD assessment was done to establish whether anti-ELTD1 antibody therapy would affect tumor-associated vasculature. Representative lectin IHC images for each treatment group are shown in Fig. 4A–D. Microvessel density assessment for all treatment groups is shown in Fig. 4E, indicating that anti-ELTD1 antibody therapy significantly decreased MVD compared with untreated GL261 glioma-bearing mice ($P < .01$). MVD was also significantly decreased for either anti–c-Met ($P < .05$) or anti-VEGF ($P < 05$) therapies compared with untreated tumors. Anti-ELTD1 therapy was not found to be significantly lower than either anti–c-Met or anti-VEGF groups.

MRA was performed and analyzed for the GL261 model to assess whether anti-ELTD1 therapy would be effective against tumor-associated macrovasculature (>50 μm in diameter). Representative morphological MRIs and MRA overlays of the brain regions from comparative untreated and anti-ELTD1 GL261 glioma-bearing mice are shown in Fig. 5A–D. Figure 5E illustrates the quantitative assessment of the tumor blood volumes (mm^3) that were calculated from MRAs obtained within brain regions of GL261 glioma-bearing mice that were either untreated (mean of 21 days following GL261 cell implantation) or treated with anti-ELTD1 antibody at day 21 following GL261 cell implantation or at maximum tumor volumes, or treated with anti-VEGF at maximum tumor volumes. There was a significant decrease in total tumor blood volume in the anti-ELTD1

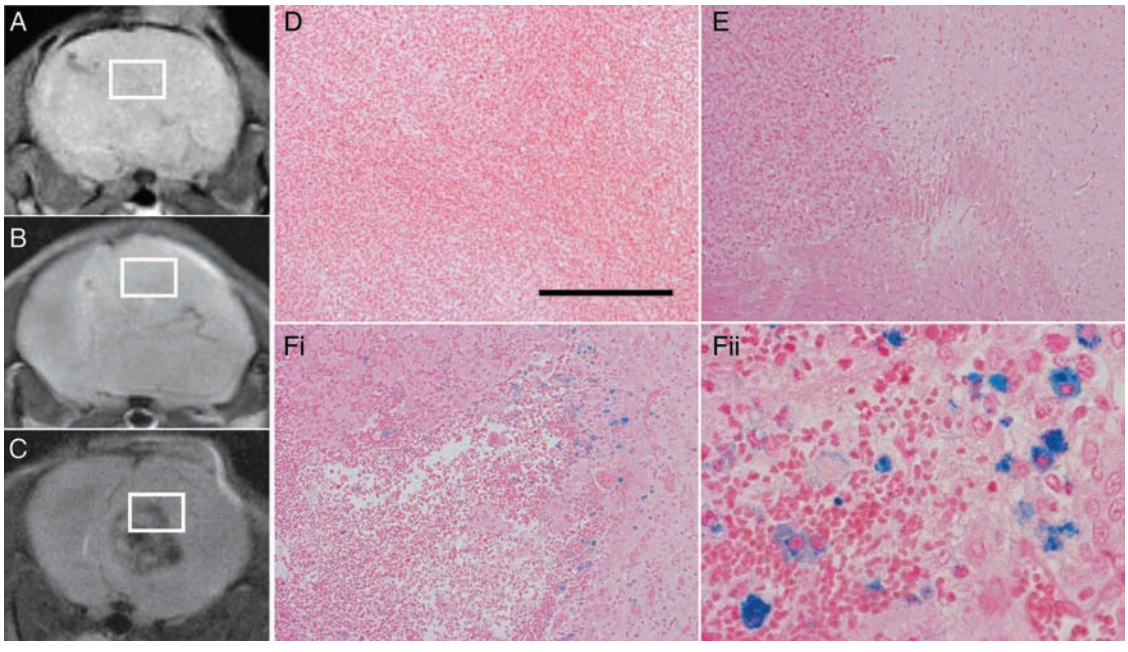

Fig. 3 Anti-ELTD1 antibody treatment has less hemorrhaging than anti-VEGF treatment in G55 gliomas. (A–C) Representative T2-weighted MRIs from G55 glioma-bearing mice that were treated with either IgG (A), anti-ELTD1 (B), or anti-VEGF (C) antibodies. Histology iron stained tissue sections from outlined regions in panels A–C from G55 tumors treated with either IgG (D), anti-ELTD1 (E), or anti-VEGF (Fi: 20 × or 60 × magnifications). Note the large areas of hemorrhaging (increased levels of iron staining) for the anti-VEGF treatment (Fi and Fii). Magnification bar = 100 μm.

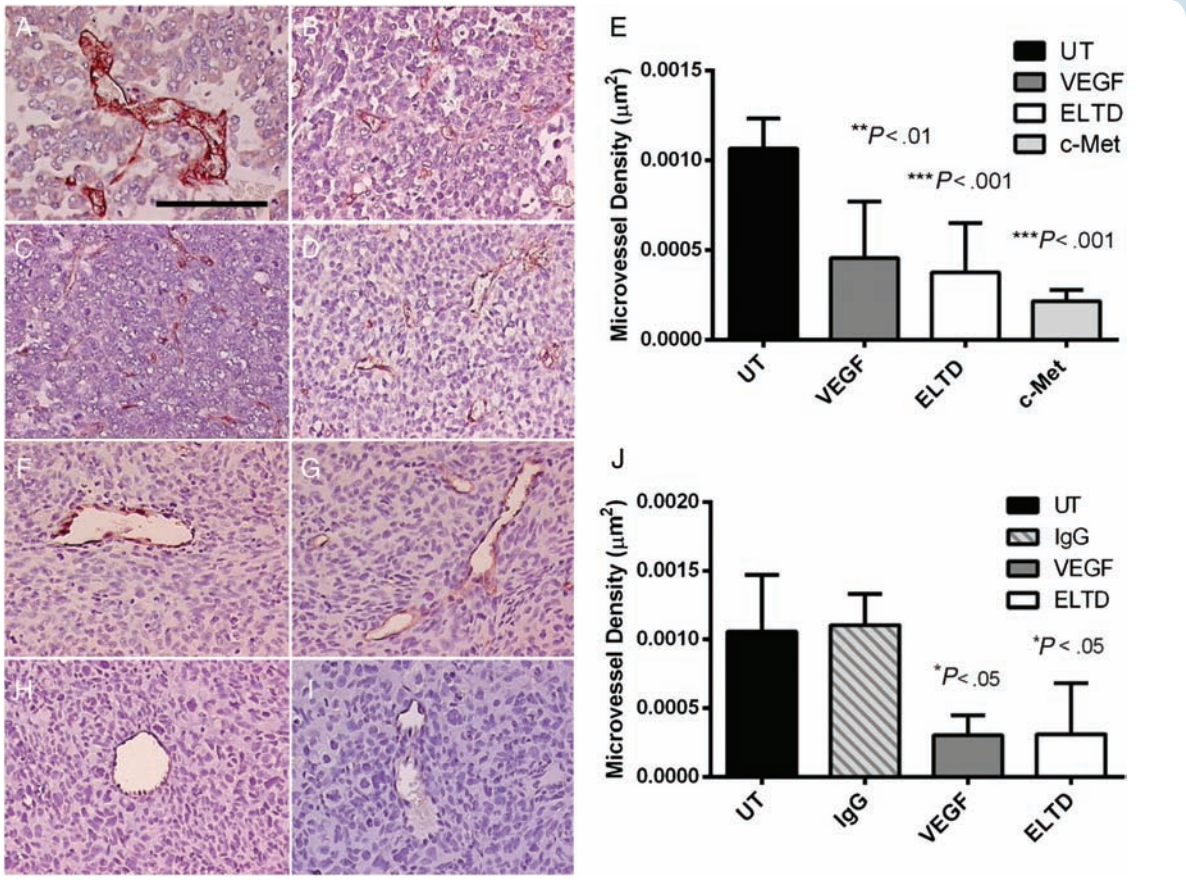

Fig. 4 Anti-ELTD1 antibody treatment decreases MVD. Representative IHC slides for CD34 obtained from GL261 (A–D) or G55 (F–H) gliomas that were either untreated (UT) (A [GL261], Fi–ii [G55]) or treated with mouse anti-VEGF (B [GL261], G [G55]), anti-ELTD1 (C [GL261], H [G55]), or anti–c-Met (D [GL261]) antibodies. Histogram of MVD for all treatment groups (UT, $n = 5$; black bar or anti-VEGF, $n = 4–5$; dark gray bar), anti-ELTD1 ($n = 5–6$; white bar), or anti–c-Met ($n = 5$; light gray bar) in GL261 (E) or G55 (J) tumors. Note darker brown staining around vessels in UT (both GL261 [A] and G55 [F]) or IgG-treated (G55 [G]) CD34 IHC samples. Significant decreases in MVD were found for only the anti-ELTD1 treatment group compared with UT mice ($P < .01$[GL261] or $P < .05$ [G55]). Anti-VEGF ($P < .01$ [GL261] or $P < .05$ [G55]) or anti–c-Met ($P < .05$ [GL261]) therapies also had significantly decreased MVD compared with UT mice. 20 × magnification for all slides. Magnification bar = 100 μm.

treatment group at 21 days following cell implantation ($P < .01$) and at maximum tumor volumes ($P < .0001$) compared with the untreated group. Anti-VEGF therapy (neither at 21 days after cell implantation [not shown] nor at maximum tumor volumes) did not significantly decrease total tumor blood volume compared with untreated mice.

MRI perfusion was conducted to establish whether anti-ELTD1 therapy would be effective against microvasculature (capillary vessels). Representative morphological MRIs and corresponding perfusion maps of brain regions from untreated and anti-ELTD1 GL261 or G55 glioma-bearing mice are shown in Fig. 6A–D and F–K, respectively. The untreated mice had a characteristic decrease in rCBF in the tumor regions (see Fig. 6B and G), whereas the anti-ELTD1 treated mice (at maximum tumor volumes) had rCBF values that were similar to the contralateral brain (see Fig. 6D and I). Figure 6E and L illustrates the quantitative assessment of the differences in tumor rCBF values (obtained between late and early tumor development and normalized to the contralateral region) calculated from MR perfusion maps obtained within brain regions of GL261 or G55 glioma-bearing mice, respectively, that were either untreated or treated with anti-ELTD1 or anti-VEGF antibody. There was a significant decrease in the differences in rCBF values in the anti-ELTD1 treatment group ($P < .0001$) and the anti-VEGF treatment group ($P < .001$) compared with the untreated group in the GL261 model, but only for the anti-ELTD1 group versus untreated ($P < .01$) or IgG-treated mice ($P < .05$) for the G55 model.

Discussion

This study focuses on the observation that antibodies to ELTD1 inhibit the growth of mouse GL261 and human G55 xenograft gliomas. It was observed that ELTD1 protein expression was found to be significantly higher in GL261 and G55 glioma tissue ($P < .01$) compared with contralateral normal brain tissue (Fig. 1). Regarding treatment response,

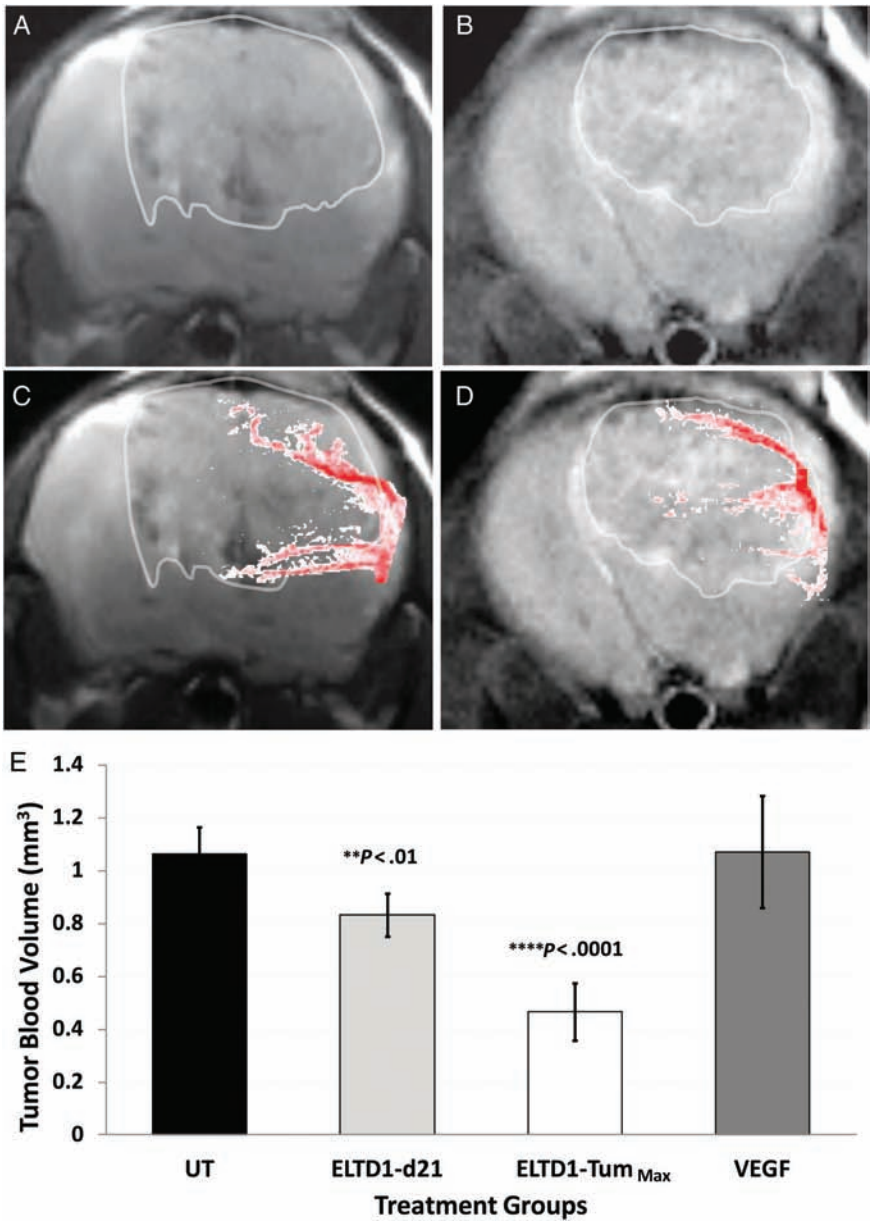

Fig. 5 Anti-ELTD1 antibody therapy decreases tumor blood volume in a mouse GL261 glioma model. (A, B) Representative T2-weighted MRIs from either untreated (UT) (A) or ELTD1 (ELTD) antibody treated (B) GL261 glioma-bearing mice. (C, D) Representative MRAs overlaid on T2-weighted MRIs from either UT (C) or ELTD antibody treated (D) GL261 glioma-bearing mice (21 days following GL261 cell implantation). (E) Histogram of tumor blood volumes (mm^3) measured from MRAs obtained from GL261 glioma-bearing mice from either UT mice (at 21 days following cell implantation) or mice treated with antibodies against ELTD (at 21 days following cell implantation or at maximum tumor volumes [26–31 days following cell implantation]) or VEGF (at maximum tumor volumes [26–31 days following cell implantation]). There was a significant decrease in tumor blood volumes for the ELTD-treated mice at 21 days following cell implantation ($P < .01$) and at maximum tumor volumes ($P < .0001$) compared with UT animals. There was no significant difference in tumor blood volumes for anti-VEGF therapy (at maximum tumor volumes) compared with UT tumors.

our data show that multiple intravenous injections of anti-ELTD1 antibodies lead to a significant decrease in tumor volumes and an increase in animal survival (Fig. 2). Given a lifespan factor of 37.5 between mice and humans,[30–32] the extra 7–10 days in survival time gained by anti-ELTD1 therapy would translate into approximately a year for humans. Furthermore, the magnitude of the effect from this unoptimized polyclonal antibody is similar to, if not slightly better than, that achieved by a mouse monoclonal anti-VEGF antibody (humanized version of bevacizumab [Avastin]) in GL261 tumors or Avastin in G55 gliomas. Another group recently found that microRNA-139-5p acts as a tumor suppressor in glioblastomas by targeting ELTD1 and regulating the cell cycle.[33]

In particular, anti-ELTD1 therapy was found to significantly decrease MVD compared with untreated tumors (Fig. 4) and

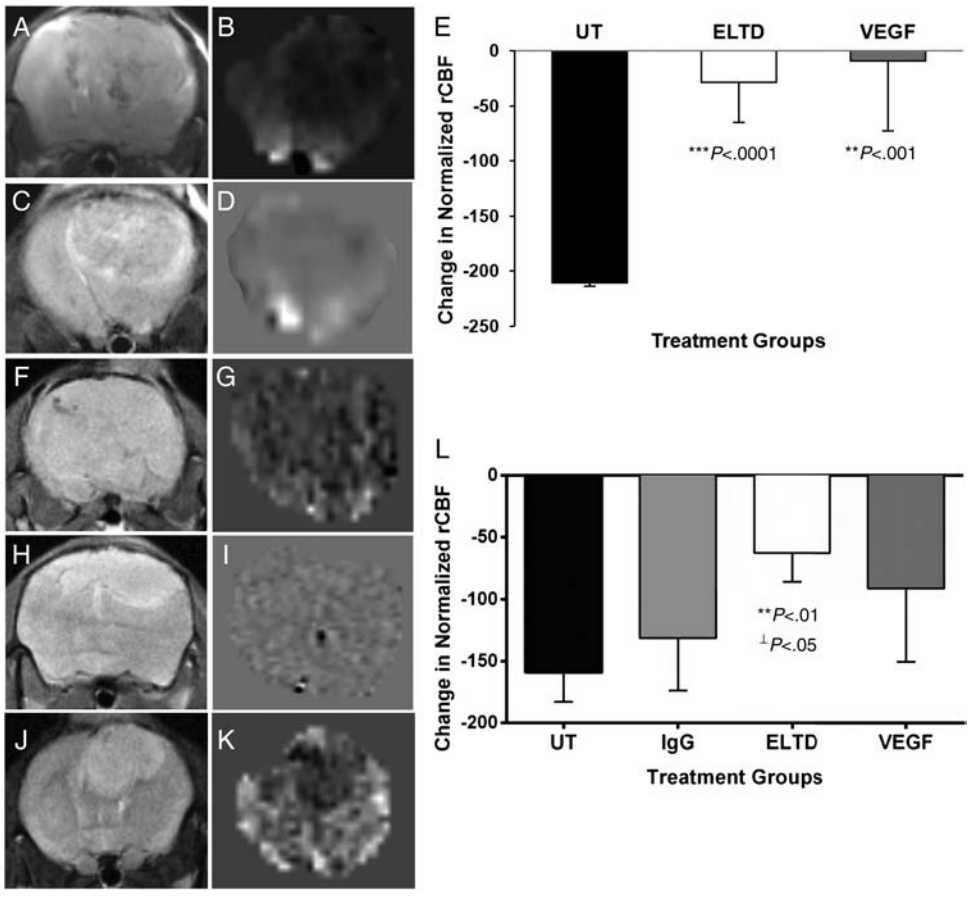

Fig. 6 Anti-ELTD1 antibody therapy alters tumor-associated vascularity as measured by MRI perfusion. Representative T2-weighted MRIs from GL261 (A, C) or G55 (F, H, J) glioma-bearing mice either untreated (UT) (A or F) or ELTD1 (ELTD) (C or H) or VEGF (J) antibody treated. Representative MR perfusion maps from either GL261 (B, D) or G55 (G, I, K) glioma-bearing mice, either UT (B or G) or ELTD (D or I) or VEGF (K) antibody treated. Normalized (against muscle tissue) tumor rCBF differences at late to early time periods for tumor growth measured from MR perfusion images obtained from GL261 (E) or G55 (L) glioma-bearing mice from either UT mice or mice treated with IgG or antibodies against ELTD or VEGF. There was a significant decrease in tumor rCBF for the ELTD-treated mice ($P < .0001$ [GL261] or $P < .01$ [G55]), as well as with VEGF-treated mice ($P < .001$ [GL261]) compared with UT animals. ELTD-treated mice also had a significant decrease in rCBF in G55 gliomas ($P < .05$) compared with IgG-treated tumors. VEGF-treated mice did not have a significant difference (eg, note decreased perfusion for VEGF [panel K]) compared with IgG-treated mice.

was just as effective as anti-VEGF therapy. Our GL261 angiography results indicated that anti-ELTD1 antibody therapy was effective in reducing tumor macrovascularity (>50 μm in diameter), whereas anti-VEGF antibody therapy had no significant effect (Fig. 5). Regarding the use of perfusion imaging to assess microvascularity, anti-ELTD1 antibody therapy was found to be quite effective in reducing tumor-related microvascularity, and this therapy seemed to be more effective than anti-VEGF therapy, particularly in the G55 model (Fig. 6). It seems that anti-VEGF therapy, unlike anti-ELTD1, seems to not be effective against macrovascularity and mainly alters microvascularity in gliomas. With the use of MRA and dynamic contrast enhanced MRI by other investigators, it was determined that bevacizumab/paclitaxel combined therapy did not block the blood supply to an MCF-7 (Michigan Cancer Foundation 7) breast tumor xenograft in severe combined immunodeficient mice, which diminished any microvascular changes targeted by the anti-VEGF antibody therapy.[30] This finding is consistent with the modest survival benefits of adding bevacizumab to current treatment regimens for some types of cancers,[27] such as gliomas.[7,10]

We also found that the anti-VEGF therapy was found to increase hemorrhaging in the G55 tumors compared with other treatments (Fig. 3). It is well known that bevacizumab (Avastin) causes intracranial hemorrhaging as a potential serious adverse event in >10% of glioblastoma multiforme patients with this treatment[34–36] and that anti-VEGF therapy has been associated with reports of hemorrhaging in other tissues.[37,38] Perhaps anti-ELTD1 antibody therapy may be more beneficial, as we did not observe this adverse event in the histological or MR images in the GL261 or G55 glioma model data compiled in this study. Although, since some of the reports for anti-VEGF therapy indicated a 10% frequency,[37] a greater sample size for anti-ELTD1 therapy may be required to confirm our finding.

Our bioinformatics analysis suggests that ELTD1 is induced in angioblasts, regions of neovascularization, and not in normal tissue,[22] further indicating that this

molecular target may be ideal for anti-angiogenic therapy. Reports by Masiero et al,[39] Favara et al,[40] and Serban et al[41] also support our data that ELTD1 is a key regulator of angiogenesis. Unfortunately, the current published data on ELTD1 function, its ligand, and structure are rather limited at this time.[41] MRA and MR perfusion imaging indicated that ELTD1 was able to decrease the tumor blood vasculature (blood vessels >50 μm in diameter) (see Fig. 5) and differences in tumor rCBF values (see Fig. 6), respectively. Anti-ELTD1 antibody therapy seems to affect both macro- and microvasculature associated with tumor growth, whereas in this study anti-VEGF antibody therapy seems to affect only tumor microvasculature. The MVD data seem to also support this finding, as MVD takes into consideration both macro- and microvasculature measurements. Perhaps anti-ELTD1 therapy can be used as a potentially safer alternate anti-angiogenic therapy clinically. Anti-ELTD1 antibody therapy may also be considered to be used in combination with anti–c-Met therapy in future studies. Our data, in addition to other independent reports recently published,[39,40,42,43] suggest that ELTD1 is a promising therapeutic candidate for inhibition of angiogenesis in gliomas and quite possibly in other tumors as well.

Funding

Funding was provided by the Oklahoma Medical Research Foundation (to R.A.T.), the Chapman Foundation (to J.D.W.), and the National Institute of General Medical Sciences of the National Institutes of Health (NIH NIGMS) grant no. 5P20GM103636-02 (to J.D.W.). An Institutional Development Award (IDeA) from the NIH NIGMS, grant no. 5P20GM103639 (to K.-M.F.) for the use of the Histology and Immunohistochemistry Core at the Stephenson Cancer Center, which provided immunohistochemistry and image analysis services, also assisted with funding.

Conflict of interest statement. None of the authors have any conflict of interest.

References

1. American Cancer Society: Cancer Facts and Figures 2014. Available at http://www.cancer.org/acs/groups/content/@research/documents/webcontent/acspc-042151.pdf. Atlanta, GA: American Cancer Society; 2014. Last accessed March 26, 2014.
2. Ostrum QT, Gittleman H, Liao P et al. CBTRUS statistical report: primary brain and central nervous system tumors diagnosed in the United States in 2007–2011. *Neuro Oncol*. 2014;16(S4):iv1–iv63.
3. Dolecek TA, Propp JM, Stroup NE et al. CBTRUS (Central Brain Tumor Registry of the United States) statistical report: primary brain and central nervous system tumors diagnosed in the United States in 2005–2009. *Neuro Oncol*. 2012;14(S5):v1–v49.
4. Porter KR, McCarthy BJ, Freels S et al. Prevalence estimates for primary brain tumors in the United States by age, gender, behavior, and histology. *Neuro Oncol*. 2010;12(6):520–527.
5. Jansen M, Yip S, Louis DN. Molecular pathology in adult gliomas: diagnostic, prognostic, and predictive markers. *Lancet Neurol*. 2010;9(7):717–726.
6. World Brain Tumor Statistics. Available at http://www.theibta.org/uploads/file/statistics.htm. Last accessed on May 20, 2014.
7. Beal K, Abrey LE, Gutin PH. Antiangiogenic agents in the treatment of recurrent or newly diagnosed glioblastoma: analysis of single-agent and combined modality approaches. *Radiat Oncol*. 2011;6:2.
8. Quick A, Patel D, Hadziahmetovic M et al. Current therapeutic paradigms in glioblastoma. *Rev Recent Clin Trials*. 2010;5(1):14–27.
9. Perry J, Okamoto M, Guiou M et al. Novel therapies in glioblastoma. *Neurol Res Int*. 2012;2012:428565.
10. Vredenburgh JJ, Desjardins A, Reardon DA et al. The addition of bevacizumab to standard radiation therapy and temozolomide followed by bevacizumab, temozolomide, and irinotecan for newly diagnosed glioblastoma. *Clin Cancer Res*. 2011;17(12):4119–4124.
11. Niclou SP, Fack F, Rajcevic U. Glioma proteomics: status and perspectives. *J Proteomics*. 2010;73(10):1823–1838.
12. Vidal S, Kovacs K, Lloyd RV et al. Angiogenesis in patients with craniopharyngiomas: correlation with treatment and outcome. *Cancer*. 2002;94(3):738–745.
13. Louis DN. Molecular pathology of malignant gliomas. *Annu Rev Pathol*. 2006;1:97–117.
14. The Cancer Genome Atlas (TCGA) Research Network. Comprehensive genomic characterization defines human glioblastoma genes and core pathways. *Nature*. 2008;455(7216):1061–1068.
15. Riemenschneider MJ, Jeuken JWM, Wesseling P et al. Molecular diagnostics of gliomas: state of the art. *Acta Neuropathol*. 2010;120(5):567–584.
16. Colman H, Zhang L, Sulman EP et al. A multigene predictor of outcome in glioblastoma. *Neuro Oncol*. 2010;12(1):49–57.
17. Farias-Eisner G, Bank AM, Hwang BY et al. Glioblastoma biomarkers from bench to bedside: advances and challenges. *Br J Neurosurg*. 2012;26(2):189–194.
18. Wren JD. A global meta-analysis of microarray expression data to predict unknown gene functions and estimate the literature-data divide. *Bioinformatics*. 2009;25(13):1694–1701.
19. Wren JD, Garner HR. Shared relationship analysis: ranking set cohesion and commonalities within a literature-derived relationship network. *Bioinformatics*. 2004;20(2):191–198.
20. Giles CB, Wren JD. Large-scale directional relationship extraction and resolution. *BMC Bioinformatics*. 2008; 9(Suppl 9): S11.
21. Goel R, Muthusamy B, Pandey A et al. Human protein reference database and human proteinpedia as discovery resources for molecular biotechnology. *Mol Biotechnol*. 2011;48(1):87–95.
22. Towner RA, Jensen RL, Colman H et al. ELTD1, a potential new biomarker for gliomas. *Neurosurgery*. 2013;72(1):77–91.
23. Towner RA, Jensen RL, Vaillant B et al. Experimental validation of 5 in-silico predicted glioma biomarkers. *Neuro Oncol*. 2013;15(12):1625–1634.
24. Doblas S, He T, Saunders D et al. Glioma morphology and tumor-induced vascular alterations revealed in seven rodent glioma models by *in vivo* magnetic resonance imaging and angiography. *J Magnetic Resonance Imaging*. 2010;32(2):267–275.
25. Garteiser P, Doblas S, Watanabe Y et al. Multiparametric assessment of the anti-glioma properties of OKN007 by magnetic resonance imaging. *J Magn Reson Imaging*. 2010;31(4):796–806.
26. Coutinho de Souza P, Mallory S, Smith N et al. Inhibition of pediatric glioblastoma tumor growth by the anti-cancer agent OKN-007 in orthotopic mouse xenografts. *Plos One*. 2015;10(8):e0134276.
27. Zhu W, Kato Y, Artemov D. Heterogeneity of tumor vasculature and antiangiogenic intervention: insights from MR angiography and DCE-MRI. *Plos One*. 2014;9(1):e86583.

28. Herscovitch P, Raichle ME. What is the correct value for the brain-blood partition coefficient for water? *J Cereb Blood Flow Metab*. 1985;5(1):65–69.
29. Tretiakova M, Antic T, Binder D et al. Microvessel density is not increased in prostate cancer: digital imaging of routine sections and tissue microarrays. *Hum Pathol*. 2013;44(4):495–502.
30. Wu JJ, Liu J, Chen EB et al. Increased mammalian lifespan and a segmental and tissue-specific slowing of aging following genetic reduction of mTOR expression. *Cell Rep*. 2013;4(5):913–920.
31. Dutta S, Sengupta P. Men and mice: relating their ages. *Life Sciences*. 2015Doi:10.1016/j.lfs.2015.10.025. [Epub ahead of print].
32. Raabe OG. Scaling of fatal cancer risks from laboratory animals to man. *Health Phys*. 1989;Suppl 1:419–432.
33. Dai S, Wang X, Li X et al. MicroRNA-139-5p acts as a tumor suppressor by targeting ELTD1 and regulating cell cycle in glioblastoma multiforme. *Biochem Biophys Res Commun*. 2015;467(2):204–210.
34. Narayana A, Kelly P, Golfinos J et al. Antiangiogenic therapy using bevacizumab in recurrent high-grade glioma: impact on local control and patient survival. *J Neurosurg*. 2009;110(1):173–180.
35. Vrendenburgh JJ, Desjardins A, Herndon JE et al. Phase II trial of bevacizumab and irinotecan in recurrent malignant glioma. *Clin Cancer Res*. 2007;13(4):1253–1259.
36. Parekh C, Jubran R, Erdreich-Epstein A et al. Treatment of children with recurrent high grade gliomas with bevacizumab containing regimen. *J Neuro-Oncol*. 2011;103(3):673–680.
37. Brouzas D, Koutsandrea C, Moschos M et al. Massive choroidal hemorrhage after intravitreal administratio n of bevacizumab (Avastin) for AMD followed by contralateral sympathetic ophthalmia. *Clin Ophthalmol*. 2009;3:457–459.
38. Ladas ID, Karagiannis DA, Rouvas AA et al. Safety of repeat intravitreal injections of bevacizumab versus ranibizumab: our experience after 2000 injections. *Retina*. 2009;29(3):313–318.
39. Masiero M, Simões FC, Han HD et al. A core human primary tumor angiogenesis signature identifies the endothelial orphan receptor ELTD1 as a key regulator of angiogenesis. *Cancer Cell*. 2013;24(2):229–241.
40. Favara DM, Banham AH, Harris AL. A review of ELTD1, a pro-angiogenic adhesion GPCR. *Biochem Soc Trans*. 2014;42(6):1658–1664.
41. Serban F, Artene SA, Georgescu AM et al. Epidermal growth factor, latrophilin, and seven transmembrane domain-containing protein 1 marker, a novel angiogenesis marker. *Onco Targets Ther*. 2015;8:3767–3774.
42. Dieterich LC, Mellberg S, Langenkamp E et al. Transcriptional profiling of human glioblastoma vessels indicates a key role of VEGF-A and TGFβ2 in vascular abnormalization. *J Pathol*. 2012;228(3):378–390.
43. McNamara MG, Sahebjam S, Mason WP. Emerging biomarkers in glioblastoma. *Cancers (Basel)*. 2013;5(3):1103–1119.